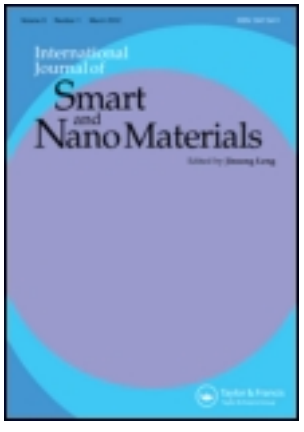

International Journal of Smart and Nano Materials
Publication details, including instructions for authors and subscription information:
http://www.tandfonline.com/loi/tsnm20

Bio-inspired robotic manta ray powered by ionic polymer-metal composite artificial muscles

Zheng Chen [a], Tae I. Um [a] & Hilary Bart-Smith [a]
[a] Department of Mechanical and Aerospace Engineering, University of Virginia, Charlottesville, VA, 22904, USA
Published online: 17 May 2012.

To cite this article: Zheng Chen , Tae I. Um & Hilary Bart-Smith (2012) Bio-inspired robotic manta ray powered by ionic polymer-metal composite artificial muscles, International Journal of Smart and Nano Materials, 3:4, 296-308, DOI: 10.1080/19475411.2012.686458

To link to this article: http://dx.doi.org/10.1080/19475411.2012.686458

International Journal of Smart and Nano Materials
Vol. 3, No. 4, December 2012, 296–308

IONIC POLYMER-METAL COMPOSITES

Bio-inspired robotic manta ray powered by ionic polymer–metal composite artificial muscles

Zheng Chen*, Tae I. Um and Hilary Bart-Smith

Department of Mechanical and Aerospace Engineering, University of Virginia, Charlottesville, VA 22904, USA

(*Received 16 December 2011; final version received 16 April 2012*)

The manta ray (*Manta birostris*) is the largest species of rays that demonstrates excellent swimming capabilities via large-amplitude flapping of its pectoral fins. In this article, we present a bio-inspired robotic manta ray using ionic polymer–metal composite (IPMC) as artificial muscles to mimic the swimming behavior of the manta ray. The robot utilizes two artificial pectoral fins to generate undulatory flapping motions, which produce thrust for the robot. Each pectoral fin consists of an IPMC muscle in the leading edge and a passive polydimethylsiloxane membrane in the trailing edge. When the IPMC is actuated, the passive polydimethylsiloxane membrane follows the bending of the leading edge with a phase delay, which leads to an undulatory flapping motion on the fin. Characterization of the pectoral fin has shown that the fin can generate flapping motions with up to 100% tip deflection and 40° twist angle. To test the free-swimming performance of the robot, a light and compact on-board control unit with a lithium ion polymer battery has been developed. The experimental results have shown that the robot can swim at 0.067 BL/s with portable power consumption of under 2.5 W.

Keywords: ionic polymer–metal composite; artificial muscle; bio-inspired robot

1. Introduction

The manta ray (*Manta birostris*, shown in Figure 1) demonstrates excellent swimming capabilities, generating highly efficient thrust via flapping of dorsally flattened pectoral fins [1]. Many efforts have been directed toward building a bio-inspired pectoral fin structure to mimic the swimming behavior of the ray. Examples include rigid plates or tensegrity structures actuated by servo motors [2–4] and flexible membrane actuated by shape memory alloy (SMA) [5]. However, these methods are not suitable for small-scale robots (of the order of 5–10 cm) [6–13] because of either the limitations in scaling or high power consumption. To construct a free-swimming and small-scale robotic manta ray, there is a need for a bio-inspired actuating material that is lightweight, compliant, resilient, and capable of generating three-dimensional (3D) deformations with portable power consumption.

Electroactive polymers, known as *artificial muscles*, can generate large deflections under an electrical stimulus [14]. Ionic polymer–metal composites (IPMCs) are an important category of ionic electroactive polymer [15–20], which can work well under a low actuation voltage (1–2 V) in a sodium salt water environment. As shown in Figure 2, an IPMC consists of one ion exchange membrane, such as Nafion (DuPont, Wilmington,

*Corresponding author. Email: zc7u@eservices.virginia.edu

ISSN 1947-542X online

http://dx.doi.org/10.1080/19475411.2012.686458
http://www.tandfonline.com

Figure 1. Bio-inspiration: The Manta Ray (courtesy: www.elasmodivec.com).

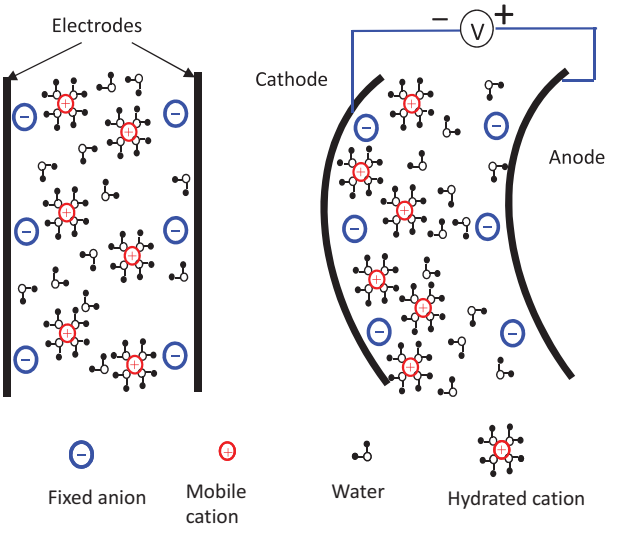

Figure 2. Actuation mechanism of IPMC [21].

DE, USA), sandwiched between two metal electrodes [16]. When the IPMC is hydrated, the positive ions in the Nafion polymer, such as sodium and calcium ions, bring water molecules and migrate to the cathode side under an electric field, whereas the negative ions are permanently fixed to the carbon chain [19]. The ion transportation and water migration introduce swelling in the cathode side and shrinking in the anode side, which eventually causes bending motion of the IPMC [19,20].

In the past, IPMC actuators have been used as a caudal fin in bio-inspired robotic fishes [6–12], where the propulsive fin mimics the bending motion observed in many biological fishes. In the propulsion mechanism of rays, undulatory flapping motions on the pectoral fin play an important role in generating highly efficient propulsion and maneuvering [1]. To fabricate an actuating membrane capable of generating complex deformations, lithography-based [22] and surface machining-based approaches [23] have been explored

to pattern the electrodes of the IPMC. To create active and passive areas in a Nafion membrane, the electrodes on the membrane were separated. By independently controlling the bending of each active area, three-dimensional deformations of the membrane have been achieved. However, the stiffness of the Nafion in the passive area limited its capability of generating large twisting motions. Punning *et al.* [13] developed pectoral fins for ray-like underwater robot by assembling separated IPMC beams with a latex foil. However, their robot did not achieve free-swimming capability because of high power consumption and low propulsion efficiency. In our previous work, an assembly-based fabrication technique was developed to integrate IPMC actuators into an artificial pectoral fin design [24]. The fin was fabricated by bonding four IPMC beams with a thin membrane of polydimethylsiloxane (PDMS). A free-swimming robotic manta ray was developed based on that pectoral fin. However, the undulation motion of the pectoral fin was not demonstrated in the free-swimming test because of complications with the implementation of on-board control system.

In this article, we present an improved bio-inspired, free-swimming robotic manta ray propelled by artificial pectoral fins. The pectoral fin consists of one IPMC artificial muscle in the leading edge and a passive PDMS membrane in the trailing edge and has the planform shape of the manta ray pectoral fin. When the IPMC is actuated, the passive PDMS membrane follows the bending of IPMC with a phase delay, which causes an undulatory motion of the fin. The pectoral fin has been characterized by key factors as they relate to the function of the robot: tip deflection, twist angle, and power consumption. As only one IPMC needs to be actuated in the pectoral fin, the control strategy is greatly simplified. To test the performance with a free-swimming robot, a light, compact on-board control unit with a lithium ion polymer battery has been developed. Experimental results have shown that the robot is capable of free swimming.

The rest of this article is organized as follows. Fabrication of artificial pectoral fin is described in Section 2. Characterization of the fin is discussed in Section 3. The design of the robotic manta ray is presented in Section 4. The free-swimming testing of the robot is illustrated in Section 5 including the snapshots of the swimming robot. The conclusion and future work are discussed in Section 6.

2. Fabrication of artificial pectoral fin

The proposed artificial pectoral fin must be able to generate undulatory motion with a twist angle as observed in the swimming of the manta ray, under hydrodynamic loads. In this article, an artificial pectoral fin was fabricated by combining IPMC actuator with a PDMS elastomer in a mold to create a predefined planform shape. The design of pectoral fin is shown in Figure 3(a). The outline shape of the fin mimics that of the manta ray. The fin is divided into two areas: IPMC beam on the leading edge and PDMS passive membrane on the trailing edge. Note that the size and shape of the IPMC are chosen to generate enough bending moment with limited power consumption. It has not been optimized yet, and will be focused in our future study.

The first step in creating the artificial pectoral fin is to fabricate the IPMC actuator. Many groups have developed different IPMC fabrication processes for various purposes [16,25–28]. In our fabrication method, we followed most of the procedure outlined by Kim and Shahinpoor [16] but added additional platinum or gold plating process to reduce the surface resistance of the electrodes [25]. A Nafion (Nafion^{TM} N1110, DuPont) membrane was selected as the ion exchange membrane in IPMC. After the electroless plating processes, about 6-μm-thick platinum electrodes have been deposited on the Nafion surfaces

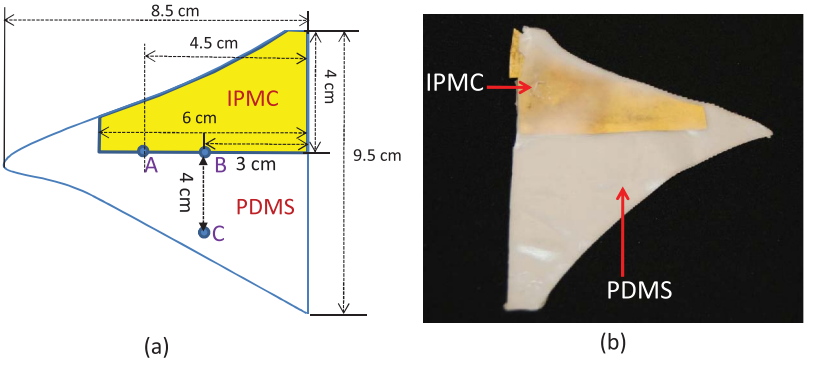

Figure 3. IPMC-powered artificial pectoral fin. (a) Pectoral fin design and (b) fabricated pectoral fin.

with good polymer–metal adhesion. To further improve the conductance of electrodes, about 1-μm-thick gold was deposited on the surface via electroplating process. The sample was then submerged in a sodium solution (1 N) for one day to exchange H^+ with Na^+ to enhance the actuation performance of the IPMC.

After fabrication of the IPMC actuator, the next step is to bond the IPMC with a PDMS elastomer membrane. The PDMS bonding process (shown in Figure 4) is described in the following five steps. (1) A Delrin polymer (McMaster, Elmhurst, IL, USA) mold was made using a Computer Numerical Control (CNC) rapid milling machine (MDX-650, Roland, Hamamatsu, Japan). The mold has two concaved areas to house the PDMS passive membrane and IPMC actuator. The thicknesses of the PDMS membrane and IPMC are 600 and 280 μm, respectively. (2) The IPMC was cut into the shape shown in Figure 3(a). (3) About 3% glass bubbles (Glass bubble K37, 3M Inc., St. Paul, MN, USA) were added into PDMS gel (Ecoflex 0030, Smooth-on Inc., Easton, PA, USA) to gain a neutrally buoyant

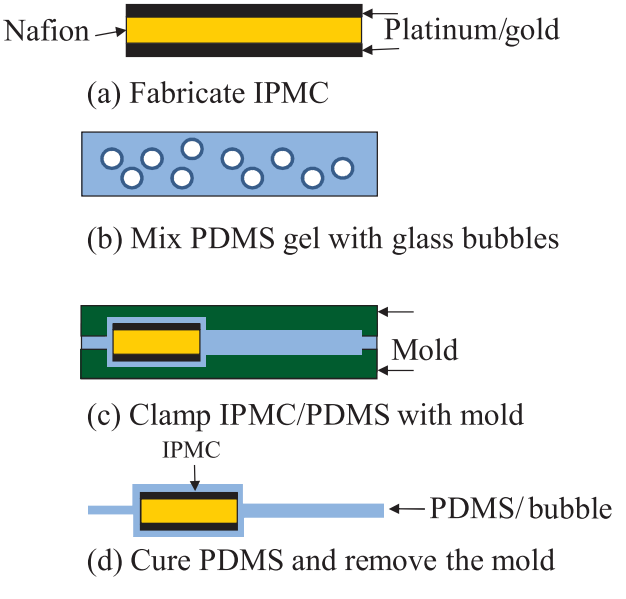

Figure 4. Fabrication process of pectoral fin.

pectoral fin. (4) The IPMC and the PDMS gel were then clamped with the mold, and the PDMS was cured at room temperature for 3 h. (5) The IPMC/PDMS artificial pectoral fin (shown in Figure 3(b)) was removed from the mold. Note that there is about 150-μm-thick PDMS covered on the top of IPMC to guarantee good bonding between passive and active areas. The additional layer of PDMS stiffens the IPMC active area. However, as the PDMS (Ecoflex) is a super soft material (Young's modulus 0.06 MPa), compared to the Nafion (Young's modulus 114 MPa), the stiffening effect is ignorable.

3. Characterization of pectoral fin

The pectoral fin was characterized in terms of tip deflection, twist angle, and power consumption. These characteristics are useful in providing comparison data in the design of the bio-inspired robot. To characterize the actuating response of the pectoral fin, three testing points (A, B, and C) are defined on the membrane (shown in Figure 3(a)).

3.1. Tip deflection measurement

To measure the tip deflection, the fin was actuated in a transparent tank containing water. A laser sensor (OADM 20I6441/S14F, Baumer Electric, Frauenfeld, Switzerland) was fixed outside the tank to measure the bending displacement at point A. Note that due to large deflection of the fin, the laser sensor was unable to capture the bending displacement of the tip. So, we moved the measurement point from the tip to the point A. The tip deflection was normalized by dividing the bending displacement by the length at the point A. Figure 5 shows the tip deflection when a square-wave actuation voltage (0.09 Hz, 4 V) was applied to the IPMC. It shows a peak-to-peak deflection of 100% in the spanwise direction. One can achieve a larger deflection by applying a higher actuation

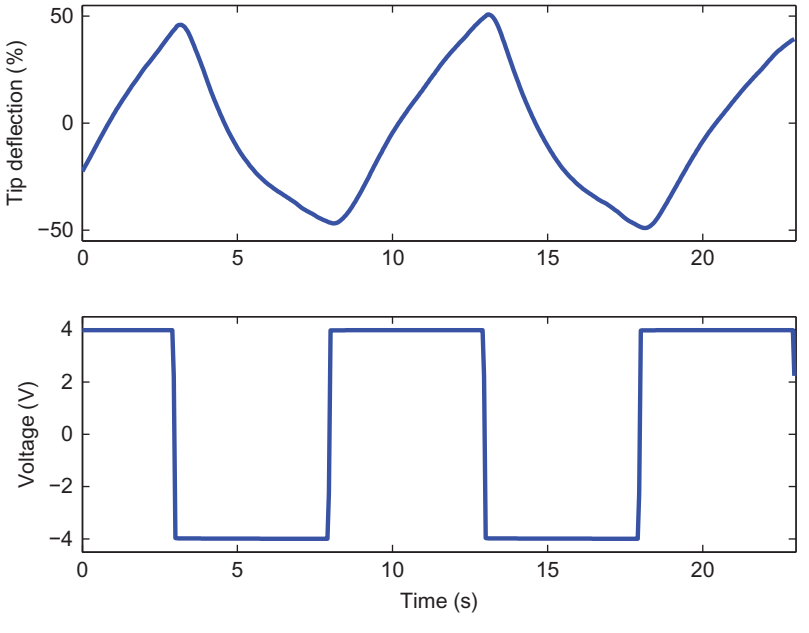

Figure 5. Tip deflection of pectoral fin.

voltage. However, there is a limit to the size of voltage applied across the IPMC – anything greater than 6 V risks dielectric breakdown through the IPMC [15].

3.2. *Bode plot of the pectoral fin*

To capture the Bode plot of the pectoral fin, a series of sinusoidal actuation signals with an amplitude of 4 V and frequencies ranging from 0.05 to 0.9 Hz were applied to the IPMC. The tip deflection at the point B and the actuation voltage were measured. The magnitude and phase shift of the tip deflection over the actuation voltage were calculated. The Bode plot (Figure 6) demonstrates that the actuation dynamics of the pectoral fin behaves as a low-pass filter with 0.4-Hz cutoff frequency. This is to be expected as the ions in the IPMC cannot move very rapidly [19].

3.3. *Characterization of twisting motion*

In order to characterize the 3D kinematics of the fin, two laser sensors (OADM 20I6441/S14F, Baumer Electric) were used to measure the bending displacements at the points B and C, d_B and d_C, respectively. The twist angle was calculated as

$$\alpha = \text{atan}\frac{d_B - d_C}{BC}, \tag{1}$$

where BC = 20 mm.

A series of square-wave voltage signals were generated via LabView (National Instruments, Austin, TX, USA), amplified using power amplifiers, and then applied to the IPMC actuator. All signals have the same amplitude of 4 V but varying frequencies from 0.06 to 1 Hz. As the IPMC actuator is being used to generate thrust in underwater

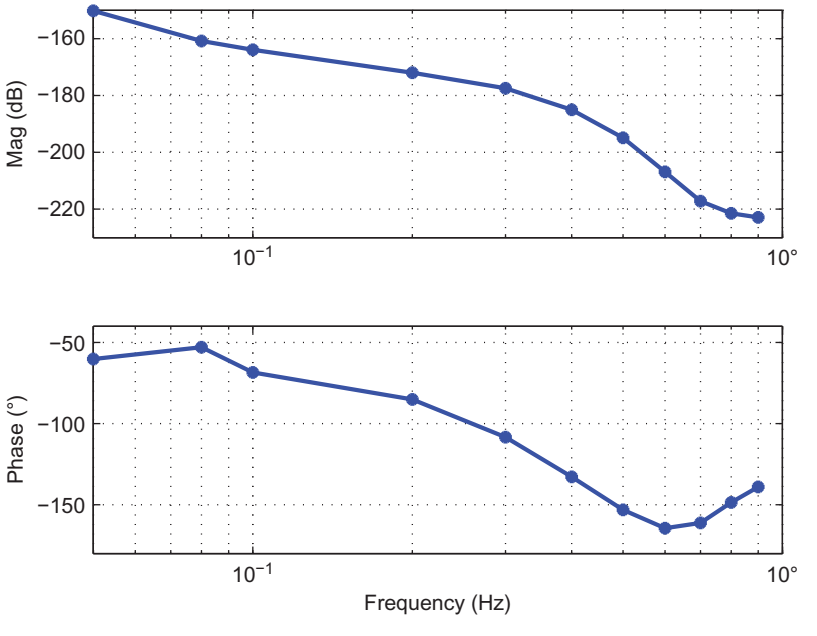

Figure 6. Bode plot of pectoral fin.

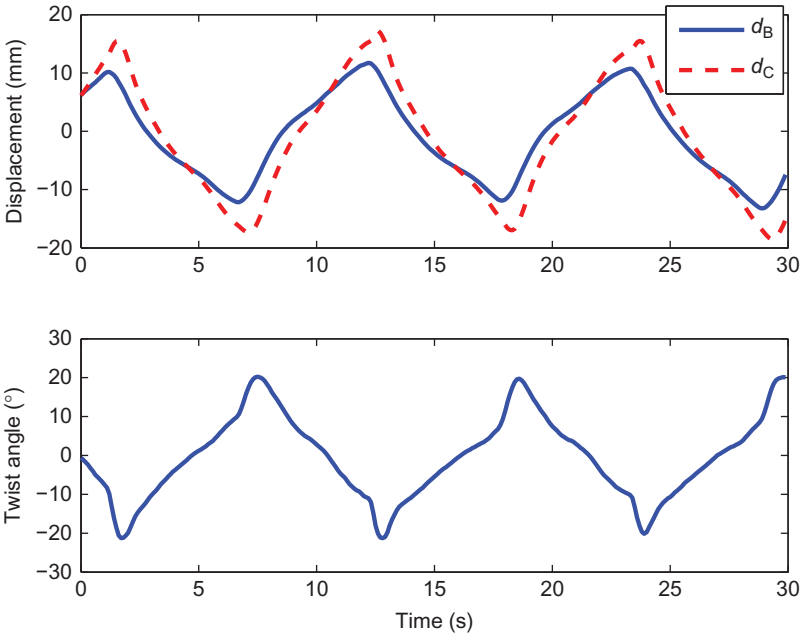

Figure 7. Twisted flapping motion on the fin.

vehicles, the 3D kinematics was quantified in water. The fin was placed in a water tank and the laser sensors were fixed outside of the tank. Figure 7 shows the undulatory flapping motion on the fin at $f = 0.09$ Hz. The upper figure shows the bending displacements, d_B and d_C, which indicates a phase delay and an amplified magnitude between the bending motions at the points B and C. The lower figure shows the calculated twist angle. The peak-to-peak twist angle is 40°, which is approximately two times larger than the value in our previous work [24]. Figure 8 shows the plot of twist angle versus operating frequency.

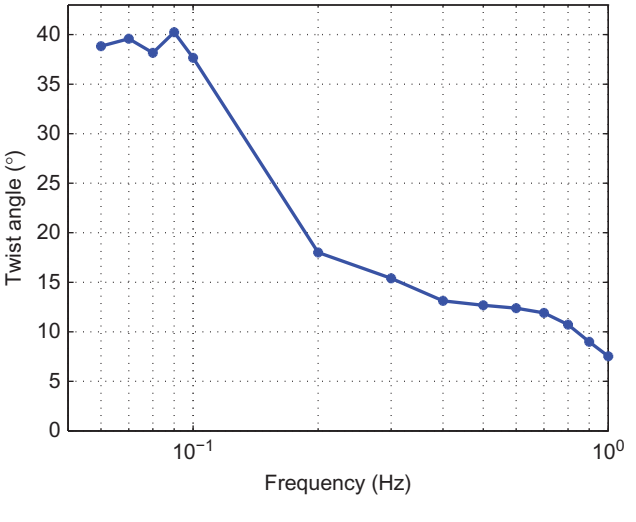

Figure 8. Twist angle versus operating frequency.

The twist angle decreases as the frequency increases. The cutoff frequency of twist angle is around 0.1 Hz. As the twist angle plays an important role in generating a thrust, the optimal operating frequency of the robot will be set around 0.1 Hz.

3.4. Power consumption

For the untethered bio-inspired robot applications, key questions regarding power consumption and optimal power management must be addressed. In this section, we study the power consumption of the pectoral fin under a square-wave actuation voltage, which is easy to generate on-board. The power consumed by the IPMC was calculated using the following equation:

$$P = \frac{1}{T}\int_0^T i\,(t)v\,(t)\,\mathrm{d}t, \tag{2}$$

where $i(t)$, $v(t)$, and T are the measured actuation current, voltage, and period, respectively. A 4-V, 0.1-Hz square-wave voltage was applied to the IPMC of the pectoral fin, which was fixed under water. Figure 9 shows the actuation voltage and current. The power consumption at 0.1 Hz is 1.09 W. Under an electrical voltage signal, the IPMC behaves as a pseudo-capacitor. When the applied voltage changes its polarization, the current reaches its peak and then drops down to a steady-state current. The steady-state current is due to the DC resistance of the polymer and the water electrolysis on the electrodes. To reduce the power consumption of the pectoral fin, it would be better to eliminate the water electrolysis by coating a waterproof protecting layer on the IPMC, which will be our future focus.

To study the relationship between power consumption and operating frequency, a series of square-wave actuation signals with an amplitude of 4 V and frequencies ranging from 0.1 to 1 Hz were applied to the fin. Figure 10 shows the power consumption versus

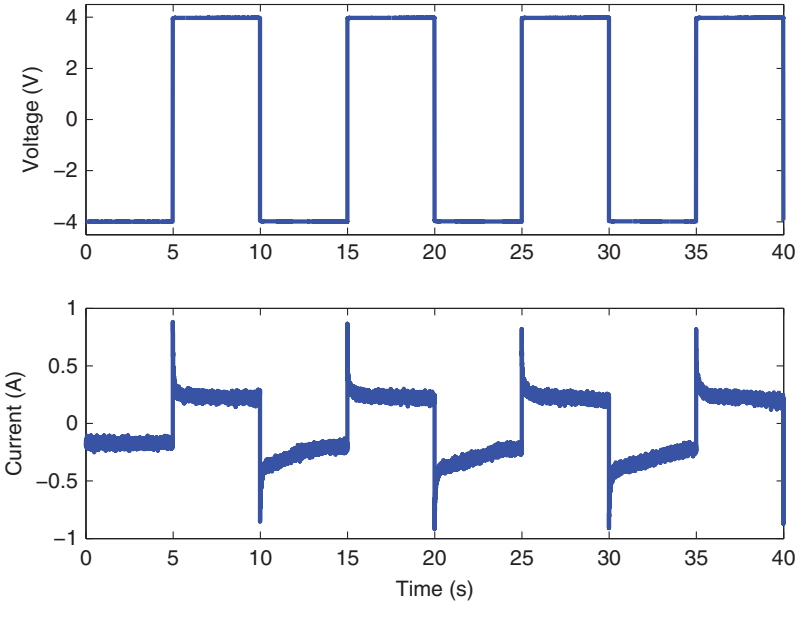

Figure 9. Actuation current and voltage under a 0.1-Hz square-wave signal.

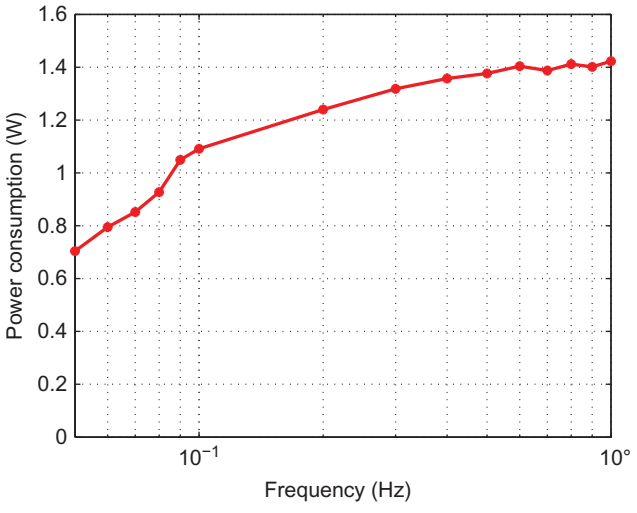

Figure 10. Power consumption versus operating frequency.

operating frequency. It demonstrates that they are positively related and the power consumption is below 1.5 W.

4. Design of robotic manta ray

In our previous work, a free-swimming and IPMC-enabled robotic manta ray was developed for the first time [24]. We used four IPMC beams bonded with thin PDMS membrane to create artificial pectoral fin. By independently controlling the bending of each IPMC beam, the fin can generate undulatory motions. However, in the free-swimming test of the robot, only a flapping motion was generated due to the complexity of generating the four control signals on-board. In this article, we present an IPMC-enabled robotic manta ray capable of free swimming. As there is only one IPMC beam in the leading edge, a single signal is needed to be generated on-board, greatly simplifying the control strategy.

4.1. Control circuit

The on-board circuit, which was developed in our previous work [24], provided a square-wave voltage signal to the IPMC actuator in the pectoral fin. Figure 11(a) shows the schematic of the circuit. A 555 timer was used to generate a frequency-adjustable square wave. The amplitude of the voltage signal, V_p, was controlled by an adjustable voltage regulator. An H-bridge driver was used to draw up to 2 A output peak current. A rechargeable 7.3-V lithium ion polymer battery (400 mAh, AA Portable Power Corp., Richmond, CA, USA) was selected as the power source for the robot. Figure 11(b) shows the picture of printed circuit board (PCB) and battery.

4.2. Free-swimming robot design

Figure 12 shows the overall shape of the robot. Two acrylic frames with gold electrodes were made to clamp the artificial wings to the body support. Gold electrodes were used to minimize corrosion. Polymer foam was placed in the middle of the frame to make the robot slightly positively buoyant. A simple hinged plastic box was used to house the circuit

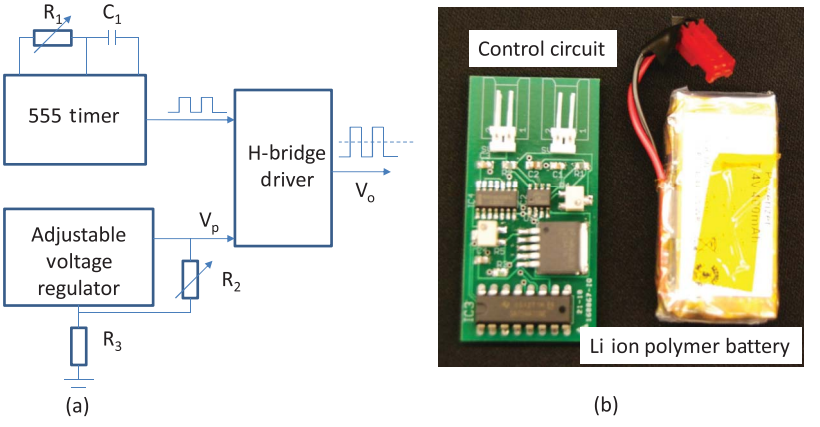

Figure 11. Control circuit and battery [24]. (a) Schematic of circuit board and (b) picture of board and battery.

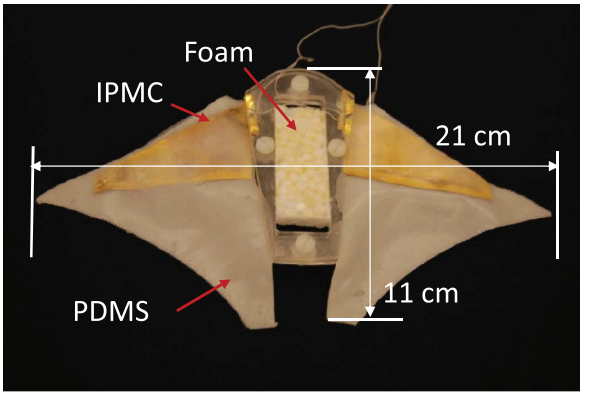

Figure 12. Robotic manta ray body.

board and battery. Once closed, only two wires were exposed outside the box. PDMS was used to seal the box waterproof. The plastic box was then glued on the top of the robot. When the robot was put under the water, the cover of the box was above the water level; thus, water could not leak into the box. The fully assembled robot was 11 cm long, 21 cm wide, and 2.5 cm thick with a mass of 55 g. The free-swimming robot with the control unit is shown in Figure 13. The total cost of the robot is about $200.

5. Free-swimming test

The robot was tested in a water tank (1.5 m wide, 4.7 m long, and 0.9 m deep). The robot was positively buoyant. The operating frequency of the square-wave actuation voltage was tuned to 0.167 Hz and the amplitude was set to 4 V. As each pectoral fin consumed less than 1.2 W (shown in Figure 10), the overall power consumption of the robot was under 2.5 W. A digital video camera (VIXIA HG21, Canon, Tokyo, Japan) was used to capture the motion of the swimming robot (see video in supplementary material, online only).

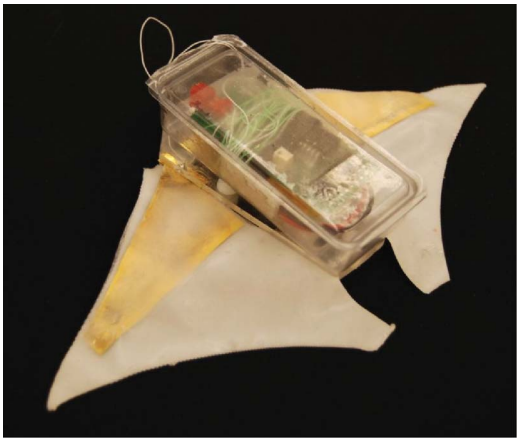

Figure 13. Free-swimming robotic manta ray.

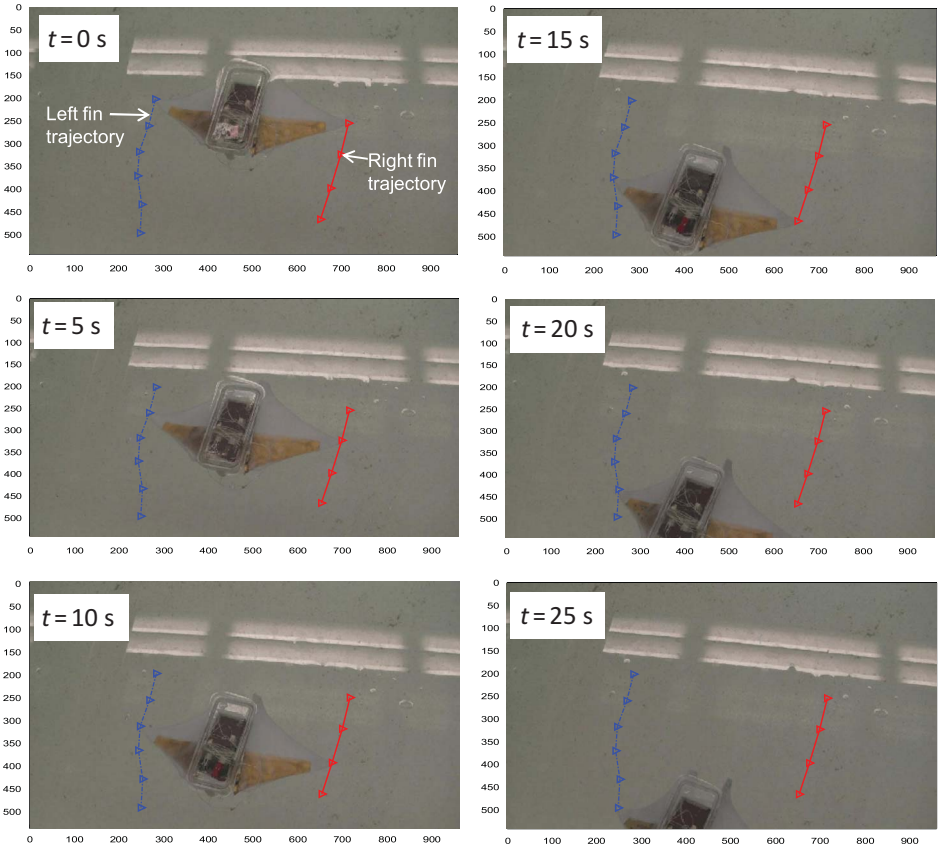

Figure 14. Snapshots of free-swimming robotic manta ray.

Figure 14 presents six snapshots of the swimming robot from top view, where the trajectories of left and right fins are plotted in blue and red, respectively. Each snapshot was taken every 5 s. A swimming speed of 0.74 cm/s was calculated from the movie using

Table 1. Comparison of ray-like robots.

Reported article	Speed (BL/s)	Power (W)	Weight (g)	Actuator
This article	0.067	2.5	55	IPMC
Punning *et al.* [13]	0.038	2.2	60	IPMC
Zhou *et al.* [2]	0.8	10.8	7300	Servo motor
Wang *et al.* [5]	0.43	Not given	354	SMA

the Edge Detection program in the LabView. As the body length was 11 cm, the speed in body length per second (BL/s) was 0.067. The comparison of ray-like swimming robots is shown in Table 1. It indicates that the IPMC-powered ray-like robots are lighter and consume less power than the robots actuated by servo motor or SMA. But they swim at lower speed.

6. Conclusion and future work

In this article, a bio-inspired robotic manta ray propelled by IPMC artificial pectoral fins has been developed. The artificial pectoral fin was fabricated by combining an IPMC actuator with a PDMS elastomer membrane. The fin was characterized in terms of tip deflection, twist angle, and power consumption. The test results have shown that the pectoral fin was able to generate up to 100% tip deflection and 40° twist angle. Based on the fabricated artificial fins, a small, free-swimming robotic manta ray has been developed. Experimental results show that the robot swam at 0.067 BL/s with portable power consumption under 2.5 W. There is large room for improvement on the swimming speed of the robot.

In our future work, we will improve the robot design in the following two aspects. First, kinematic and dynamic models of the manta ray will be developed. This will help us to understand the propulsion mechanism of biological manta ray and provide a useful framework on how to optimize the design and control the pectoral fin. Second, the pectoral fin will be optimally designed to improve the propulsion efficiency and speed.

Acknowledgments

This research was supported in part by the Office of Naval Research (ONR) under the Multidisciplinary University Research Initiative (MURI) Grant N00014-08-1-0642 and the David and Lucille Packard Foundation.

References

[1] L.J. Rosenberger, *Pectoral fin locomotion in batoid fishes: Undulation versus oscillation*, J. Exp. Biol. 204 (2001), pp. 379–394.
[2] C. Zhou and K.H. Low, *Design and locomotion control of a biomimetic underwater vehicle with fin propulsion*, IEEE/ASME Trans. Mechatron. 17 (2012), pp. 1–30.
[3] K. Moored, W. Smith, J. Hester, W. Chang, and H. Bart-Smith, *Investigating the thrust production of a myliobatoid-inspired oscillating wing*, Adv. Sci. Technol. 58 (2008), pp. 25–30.
[4] K. Moored and H. Bart-Smith, *Investigation of clustered actuation in tensegrity structures*, Int. J. Solids Struct. 46 (17) (2009), pp. 3272–3281.
[5] Z. Wang, Y. Wang, J. Li, and G. Hang, *A micro biomimetic manta ray robot fish actuated by SMA*, Proceedings of the 2009 IEEE International Conference on Robotics and Biomimetics, Guilin, China, 19–23 December 2009, pp. 1809–1813.
[6] S. Guo, T. Fukuda, and K. Asaka, *A new type of fish-like underwater microrobot*, IEEE/ASME Trans. Mechatron. 8 (1) (2003), pp. 136–141.

[7] M. Shahinpoor, *Conceptual design, kinematics and dynamics of swimming robotic structures using active polymer gels*, Proceedings of the ADPA/AIAA/ASME/SPIE Conference on Active Materials & Adaptive Structures, Alexandria, VA, 1991.
[8] M. Shahinpoor, *Conceptual design, kinematics and dynamics of swimming robotic structures using ionic polymeric muscles*, Int. J. Smart Mater. Struct. 1 (1) (1992), pp. 91–94.
[9] G. Chamorro, *Swimming robotic structures equipped with IPMC artificial muscles*, Master thesis, Department of Mechanical Engineering, University of New Mexico, Albuquerque, NM, 2000.
[10] M. Mojarrad and M. Shahinpoor, *Noiseless propulsion for swimming robotic structures using polyelectrolyte ion-exchange membranes*, Proceedings of the SPIE 1996 North American Conference on Smart Structures and Materials, San Diego, CA, Vol. 2716, Paper No. 27, 1996.
[11] M. Mojarrad, *Study of ionic polymeric gels as smart materials and artificial muscles for biomimetic swimming robotic applications*, Ph.D. diss., Department of Mechanical Engineering, University of New Mexico, Albuquerque, NM, 2001.
[12] X. Tan, D. Kim, N. Usher, D. Laboy, J. Jackson, A. Kapetanovic, J. Rapai, B. Sabadus, and X. Zhou, *An autonomous robotic fish for mobile sensing*, Proceedings of the IEEE/RSJ International Conference on Intelligent Robots and Systems, Beijing, China, 9–15 October 2006, pp. 5424–5429.
[13] A. Punning, M. Anton, M. Kruusmaa, and A. Aabloo, *A biologically inspired ray-like underwater robot with electroactive polymer pectoral fins*, Proceedings of the 2004 IEEE International Conference on Mechatronics and Robotics, Aachen, Germany, 21–24 September 2004, pp. 241–245.
[14] Y. Bar-Cohen, *Electroactive polymers as artificial muscles – Capabilities, potentials and challenges*, in *Handbook on Biomimetics*, Y. Osada, ed., NTS Inc., Bakersfield, CA, 2000, pp. 1–13.
[15] M. Shahinpoor and K. Kim, *Ionic polymer–metal composites: I. Fundamentals*, Smart Mater. Struct. 10 (2001), pp. 819–833.
[16] K.J. Kim and M. Shahinpoor, *Ionic polymer–metal composites: II. Manufacturing techniques*, Smart Mater. Struct. 12 (2003), pp. 65–79.
[17] M. Shahinpoor and K. Kim, *Ionic polymer–metal composites. Part IV. Industrial and medical applications*, Smart Mater. Struct. 14 (2005), pp. 197–214.
[18] M. Shahinpoor, K.J. Kim, and D. Leo, *Ionic polymer–metal composites as multifunctional materials*, Polym. Compos. 24 (1) (2003), pp. 24–33.
[19] S. Nemat-Nasser and J. Li, *Electromechanical response of ionic polymer–metal composites*, J. Appl. Phys. 87 (7) (2000), pp. 3321–3331.
[20] S. Nemat-Nasser, *Micromechanics of actuation of ionic polymer–metal composites*, J. Appl. Phys. 92 (5) (2002), pp. 2899–2915.
[21] Z. Chen and X. Tan, *A control-oriented and physics-based model for ionic polymer–metal composite actuators*, IEEE/ASME Trans. Mechatron. 13 (5) (2008), pp. 519–529.
[22] Z. Chen and X. Tan, *Monolithic fabrication of ionic polymer–metal composite actuators capable of complex deformation*, Sens. Actuators A Phys. 157 (2) (2010), pp. 246–257.
[23] K.J. Kim, D. Pugal, and K.K. Leang, *A twistable ionic polymer–metal composite artificial muscle for marine applications*, Marine Technol. Soc. J. 45 (4) (2011), pp. 83–98.
[24] Z. Chen, T.I. Um, and H. Bart-Smith, *A novel fabrication of ionic polymer–metal composite membrane actuator capable of 3-dimensional kinematic motions*, Sens. Actuators A Phys. 168 (1) (2011), pp. 131–139.
[25] K.J. Kim and M. Shahinpoor, *A novel method of manufacturing three-dimensional ionic polymer–metal composites (IPMCs) biomimetic sensors, actuators, and artificial muscles*, Polymer 43 (2002), pp. 797–802.
[26] S.J. Kim, I.T. Lee, and Y.H. Kim, *Performance enhancement of IPMC actuator by plasma surface treatment*, Smart Mater. Struct. 16 (1) (2007), pp. N6–N11.
[27] C. Chung, P. Fung, Y. Hong, M. Ju, C. Lin, and T. Wu, *A novel fabrication of ionic polymer–metal composites (IPMC) actuator with silver nano-powders*, Sens. Actuators B Chem. 117 (2006), pp. 367–375.
[28] S.J. Lee, M.J. Han, S.J. Kim, J.Y. Jho, H.Y. Lee, and Y.H. Kim, *A new fabrication method for IPMC actuators and application to artificial fingers*, Smart Mater. Struct. 15 (5) (2006), pp. 1217–1224.